Wave-guided optical waveguides

Palima, Darwin; Bañas, Andrew Rafael; Vizsnyiczai, George; Kelemen, L.; Ormos, P.; Glückstad, Jesper

Published in:
Optics Express

Link to article, DOI:
10.1364/OE.20.002004

Publication date:
2012

Document Version
Publisher's PDF, also known as Version of record

Wave-guided optical waveguides

D. Palima,[1] A. R. Bañas,[1] G. Vizsnyiczai,[2] L. Kelemen,[2] P. Ormos,[2] and J. Glückstad[1,*]

[1]*DTU Fotonik, Dept. of Photonics Engineering, Technical University of Denmark, DK-2800, Kgs. Lyngby, Denmark*
[2]*Institute of Biophysics, Biological Research Centre, Hungarian Academy of Sciences, Szeged H-6701, Hungary*
[*] *jesper.gluckstad@fotonik.dtu.dk*
www.ppo.dk

Abstract: This work primarily aims to fabricate and use two photon polymerization (2PP) microstructures capable of being optically manipulated into any arbitrary orientation. We have integrated optical waveguides into the structures and therefore have freestanding waveguides, which can be positioned anywhere in the sample at any orientation using optical traps. One of the key aspects to the work is the change in direction of the incident plane wave, and the marked increase in the numerical aperture demonstrated. Hence, the optically steered waveguide can tap from a relatively broader beam and then generate a more tightly confined light at its tip. The paper contains both simulation, related to the propagation of light through the waveguide, and experimental demonstrations using our BioPhotonics Workstation. In a broader context, this work shows that optically trapped microfabricated structures can potentially help bridge the diffraction barrier. This structure-mediated paradigm may be carried forward to open new possibilities for exploiting beams from far-field optics down to the subwavelength domain.

OCIS codes: (170.4520) Optical confinement and manipulation; (220.4000) Microstructure fabrication; (230.7370) Waveguides.

References and links

1. A. Ashkin, "Acceleration and trapping of particles by radiation pressure," Phys. Rev. Lett. **24**, 156-159 (1970).
2. A. Ashkin, J. M. Dziedzic, J. E. Bjorkholm, and S. Chu, "Observation of a single-beam gradient force optical trap for dielectric particles," Opt. Lett. **11**, 288-290 (1986).
3. H. Misawa, K. Sasaki, M. Koshioka, N. Kitamura, and H. Masuhara, "Multibeam laser manipulation and fixation of microparticles," Appl. Phys. Lett. **60**, 310-312 (1992).
4. K. Sasaki, M. Koshioka, H. Misawa, N. Kitamura, and H. Masuhara, "Pattern formation and flow control of fine particles by laser-scanning micromanipulation," Opt. Lett. **16**, 1463-1465 (1991).
5. E. R. Dufresne and D. G. Grier, "Optical tweezer arrays and optical substrates created with diffractive optics," Rev. Sci. Instrum. **69**, 1974-1977 (1998).
6. R. L. Eriksen, P. C. Mogensen, and J. Glückstad, "Multiple-beam optical tweezers generated by the generalized phase-contrast method," Opt. Lett. **27**, 267-269 (2002).
7. A. Constable, J. Kim, J. Mervis, F. Zarinetchi, and M. Prentiss, "Demonstration of a fiber-optical light-force trap," Opt. Lett. **18**, 1867-1869 (1993).
8. F. Merenda, J. Rohner, J.M. Fournier, and R.P. Salathé, "Miniaturized high-NA focusing-mirror multiple optical tweezers," Opt. Express **15**, 6075-6086 (2007).
9. T. Čižmár, M. Mazilu, and K. Dholakia, "In situ wavefront correction and its application to micromanipulation," Nature Photon. **4**, 388-394 (2010).
10. A. Pralle, M. Prummer, E. L. Florin, E. H. Stelzer, and J. K. Hörber, "Three-dimensional high-resolution particle tracking for optical tweezers by forward scattered light," Microsc. Res. Techniq. **44**, 378-86 (1999).
11. A. Ashkin and J. M. Dziedzic, "Feedback stabilization of optically levitated particles," Appl. Phys. Lett. **30**, 202-204 (1977).
12. S. Tauro, A. Bañas, D. Palima, and J. Glückstad, "Dynamic axial stabilization of counter-propagating beam-traps with feedback control," Opt. Express **18**, 18217-18222 (2010).
13. J. T. Finer, R. M. Simmons, and J. A. Spudich, "Single myosin molecule mechanics: piconewton forces and nanometre steps," Nature **368**, 113-119 (1994).
14. K. C. Neuman and A. Nagy, "Single-molecule force spectroscopy: optical tweezers, magnetic tweezers and atomic force microscopy," Nat. Methods **5**, 491–505 (2008).
15. A. G. Banerjee, S. Chowdhury, W. Losert, and S. K. Gupta, "Survey on indirect optical manipulation of cells, nucleic acids, and motor proteins," J. Biomed. Opt. **16**, 051302 (2011).

#158363 - $15.00 USD Received 21 Nov 2011; revised 2 Jan 2012; accepted 4 Jan 2012; published 13 Jan 2012

16. F. Hajizadeh and S. N. S. Reihani, "Optimized optical trapping of gold nanoparticles," Opt. Express **18**, 551–559 (2010).
17. R.Yan, D. Gargas, and P. Yang, "Nanowire photonics," Nature Photon. **3**, 569 - 576 (2009).
18. Y. Nakayama, P.J. Pauzauskie, A. Radenovic, R.M. Onorato, R.J. Saykally, J. Liphardt, and P. Yang, "Tunable nanowire nonlinear optical probe," Nature **447**, 1098-1101 (2007).
19. P.J. Pauzauskie, A. Radenovic, E. Trepagnier, H. Shroff, P. Yang, and J. Liphardt, "Optical trapping and integration of semiconductor nanowire assemblies in water," Nature Mater. **5**, 97–101 (2006).
20. J. Plewa, E. Tanner, D. Mueth, and D. Grier, "Processing carbon nanotubes with holographic optical tweezers," Opt. Express **12**, 1978-1981 (2004).
21. J. L. Hernández-Pozos, W. M. Lee, L. I. Vera-Robles, A. Campero, and K. Dholakia, "Controlled three-dimensional manipulation of vanadium oxide nanotubes with optical tweezers," Appl. Phys. Lett. **93**, 243107 (2008).
22. L. Ikin, D. M. Carberry, G. M. Gibson, M. J. Padgett, and M. J. Miles, "Assembly and force measurement with SPM-like probes in holographic optical tweezers," New J. Phys. **11**, 023012 (2009).
23. D. M. Carberry, S. H. Simpson, J. A. Grieve, Y. Wang, H. Schafer, M. Steinhart, R. Bowman, G. M. Gibson, M. J. Padgett, S. Hanna, and M. J. Miles, "Calibration of optically trapped nanotools," Nanotechnology **21**, 175501 (2010).
24. D. B. Phillips, J. A. Grieve, S. N. Olof, S. J. Kocher, R. Bowman, M. J. Padgett, M. J. Miles, and D. M. Carberry, "Surface imaging using holographic optical tweezers," Nanotechnology **22**, 285503 (2011).
25. M.R. Pollard, S.W. Botchway, B. Chichkov, E. Freeman, R.N.J. Halsall, D.W.K. Jenkins, I. Loader, A. Ovsianikov, A.W. Parker, R. Stevens, R. Turchetta, A.D. Ward, and M. Towrie, "Optically trapped probes with nanometer-scale tips for femto-Newton force measurement," New J. Phys. **12** 113056 (2010).
26. J. Glückstad, "Manipulating microtools with nanofeatures using light in 3d real-time," Presented at the iNANO Seminar, Aarhus University, Denmark, 2 February, 2007.
27. P. J. Rodrigo, L. Gammelgaard, P. Bøggild, I. R. Perch-Nielsen, and J. Glückstad, "Actuation of microfabricated tools using multiple GPC-based counterpropagating-beam traps," Opt. Express **13,** 6899-6904 (2005).
28. P. J. Rodrigo, L. Kelemen, C. A. Alonzo, I. R. Perch-Nielsen, J. S. Dam, P. Ormos, and J. Glückstad, "2D optical manipulation and assembly of shape-complementary planar microstructures," Opt. Express **15**, 9009-9014 (2007).
29. P.J. Rodrigo, L. Kelemen, D. Palima, C. A. Alonzo, P. Ormos, and J. Glückstad, "Optical microassembly platform for constructing reconfigurable microenvironments for biomedical studies," Opt. Express **17**, 6578-6583 (2009).
30. D. F.Tan, Y. Li, F. J. Qi, H. Yang, Q. H. Gong, X. Z. Dong, and X.M. Duan, "Reduction in feature size of two-photon photo-polymerization using SCR500," Appl. Phys. Lett. **90**, 071106 (2007).
31. J. Glückstad, "Optical manipulation: Sculpting the object," Nature Photon. **5**, 7–8 (2011).
32. K. M. Davis, K. Miura, N. Sugimoto, and K. Hirao, "Writing waveguides in glass with a femtosecond laser," Opt. Lett. **21**, 1729-1731 (1996).
33. L. Tong, R. Gattass, I. Maxwell, J. Ashcom, and E. Mazur, "Optical loss measurements in femtosecond laser written waveguides in glass," Opt. Commun. **259**, 626-630 (2006).
34. A. Levskaya, O. D. Weiner, W. A. Lim, and C. A. Voigt, "Spatiotemporal control of cell signalling using a light-switchable protein interaction," Nature **461**, 997-1001 (2009).
35. K.S. Yee, "Numerical solution of initial boundary value problems involving Maxwell's equations in isotropic media," IEEE Antennas Propag. **14**, 302–307 (1966).
36. G. Van Engen, S. A. Diddams, and T. S. Clement, "Dispersion Measurements of Water with White-Light Interferometry," Appl. Opt. **37**, 5679-5686 (1998).
37. T. A. Anhøj, "Fabrication of High Aspect Ratio SU-8 Structures for Integrated Spectrometers," doctoral dissertation, Technical University of Denmark, Denmark (2007).
38. G. P. Agrawal, *Lightwave Technology: Components and Devices* (Wiley, 2004), pp. 18-19.
39. L. Kelemen, S. Valkai, and P. Ormos, "Integrated optical motor," Appl. Opt. **45**, 2777-2780 (2006).
40. H.U. Ulriksen, J. Thøgersen, S. Keiding, I. Perch-Nielsen, J. Dam, D. Z. Palima, H. Stapelfeldt, and J. Glückstad, "Independent trapping, manipulation and characterization by an all-optical biophotonics workstation," J. Europ. Opt. Soc.: Rap. Public. **3**, 080341-080345 (2008).
41. E. McLeod and C.B. Arnold, "Subwavelength direct-write nanopatterning using optically trapped microspheres," Nature Nanotech. **3**, 413–417 (2008).
42. G. Brambilla, "Optical fibre nanowires and microwires: a review," J. Opt. **12**, 043001 (2010).
43. D. K. Gramotnev and S. I. Bozhevolnyi, "Plasmonics beyond the diffraction limit," Nature Photon. **4**, 83-91 (2010).
44. P. Verma, T. Ichimura, T. Yano, Y. Saito, and S. Kawata, "Nano-imaging through tip-enhanced Raman spectroscopy: Stepping beyond the classical limits," Laser Photon. Rev. **4**, 548-561 (2010).
45. D. O'Carroll, I. Lieberwirth, and G. Redmond, "Microcavity effects and optically pumped lasing in single conjugated polymer nanowires," Nature Nanotech. **2**, 180-184 (2007).
46. F. Gu, H. Yu, P. Wang, Z. Yang, and L. Tong, "Light-emitting polymer single nanofibers via waveguiding excitation," ACS Nano **4**, 5332-5338 (2010).
47. M. Majumder, N. Chopra, R. Andrews, and B.J. Hinds, "Nanoscale hydrodynamics: Enhanced flow in carbon nanotubes," Nature **438,** 44 (2005).

#158363 - $15.00 USD Received 21 Nov 2011; revised 2 Jan 2012; accepted 4 Jan 2012; published 13 Jan 2012

1. Introduction

One way to keep track of the developments in optical trapping is to compare their novelty with Ashkin's original demonstration [1], which used a single pair of static counterpropagating beams focused by regular lenses onto a sample chamber to trap polystyrene microbeads, one at a time, while observing them through a microscope. It is now common to have single-beam trapping that reuses the same microscope objective lens [2]. We now have multiple simultaneous traps [3], with options to independently control each trap both in the single-sided and the counterpropagating/dual-beam geometries using beam manipulation techniques like time-multiplexing [4], diffractive optics [5], and Generalized Phase Contrast [6] for 3D trapping and manipulation. Instead of microscope objectives, the trapping beams may also be delivered using fibers [7] or microoptical elements custom-built onto the sample chambers themselves [8]. Trapping with minimal laser power is also possible with aberration corrections [9]. The particle position detection system [10] can serve a range of functions from simple visualization to feedback control [11,12] and quantitative optical force measurements based on the position fluctuations [13].

These technical developments in the trapping implementation (i.e., the '*how'* of optical trapping*)* enables the trapping of different types of particles (*'what'*) in a variety of working environments ('*where'*). More importantly, from a practical perspective, these developments can enable and define novel applications and purpose for optical trapping (*'why'*). The *how*, *what*, *where* and *why* of optical trapping can, together, define the novelty of optical trapping setups and experiments. For example, polystyrene microbeads have been trapped since 1970, but they can be very valuable when such bead is attached to macromolecules and trapped in a technically refined system for accurate force measurements of the molecule's mechanical properties [13]. This subfield based on quantitative optical force measurements has taken on a life of its own with active developments both in the instrumentation and the biological applications [14, 15]. However, many keep an eye out for other applications of optical trapping, since another so-called "killer application", which may not necessarily involve quantitative force measurements, could be lurking in the horizon,

Micro- and nanofabrication techniques support the search for new optical trapping applications by providing a host of novel synthetic structures that can be optically trapped [16-29]. Optical traps can transport and manipulate nanoparticles [16], nanowires [17-19], nanotubes [20,21]**,** optical probes/tools [22-27] and building blocks for microassembly [28, 29]. However, unlike microstructures that are amenable to arbitrary translational and angular positioning in 3D space (6DOF or six degree of freedom control), nanostructures are steerable only with limited angular control when using optical traps. One workaround, akin to indirect optical manipulation of biomolecules [15], is to attach the nanostructures onto spherical trapping handles [21–23]. The handles can be attached *on the fly* using optical traps onto nanotubes [21–23] and these handles can be made detachable [21] or fixed to the structure [22, 23]. Optically trapped freestanding probes open possibilities for probing arbitrary surfaces and have been demonstrated for SPM-like sideways imaging of a highly curved cell wall (*Pseudopediastrum* algae) using optically trapped diatom as probe [24]. Using our BioPhotonics Workstation, we have previously demonstrated 6DOF control of microfabricated structures [27], as well as automated assembly [28] and proof-of-principle demonstration of optically reconfigurable micro-environments [29] using 3D structures fabricated via two-photon polymerization (2PP). The three-dimensional resolution in 2PP fabrication (reported with sub-25nm feature sizes [30]) offers possibilities for creating novel structures for optical trapping [31].

In this work, we combine two-photon microfabrication and optical trapping to demonstrate "*wave-guided optical waveguides*", which uses optical waves to trap and guide the optical waveguides. We use 2PP to fabricate free-standing optical waveguides that form part of support structures equipped with trapping handles. Optical waveguides have been previously created within the bulk of transparent solid host media via femtosecond-laser-induced changes in the refractive index [32,33]. Here we present proof-of-principle demonstrations that the

#158363 - $15.00 USD Received 21 Nov 2011; revised 2 Jan 2012; accepted 4 Jan 2012; published 13 Jan 2012

free-standing waveguides can be optically trapped and manipulated using our BioPhotonics Workstation. Waveguides are indispensable in beam delivery systems designed to send and/or collect light from hard-to-reach areas (e.g. endoscopy). Our work, which uses free-standing waveguides, creates a "mobile solution" or at least a wireless phone (to use a telephony analogy) for flexible delivery of optical energy and signals in a microscopic environment that is free from the physical constraints of having a "wired device".

Section 2 presents numerical simulations of wave propagation through a bent polymer wire in aqueous medium (simulating a free-standing, two-photon-polymerized waveguide). We also describe the fabrication of such a waveguide, equipped with handles for optical trapping, via two-photon polymerization in this section. Section 3 presents proof-of-principle experiments showing light guiding through optically trapped and manipulated waveguides, where we also show selective fluorescence excitation of a bead among a vertical stack. We additionally demonstrate reverse propagation through the waveguide, showing potential for guiding off-axis-directed light from a localized source and redirecting it to the microscope objective. Finally, we present conclusions and perspectives in Section 4.

2. Design and fabrication of optically steerable free-standing waveguides

A possible scenario for using optically steerable waveguides is illustrated in Fig. 1(b), where an artist rendition zooms into a microscopic chamber containing such waveguides, held by red optical trapping beams, in the vicinity of a relatively large cell (e.g., a mammalian cell, which can be tens of microns in size). Here the goal is to selectively illuminate a localized target (e.g., light-switchable proteins [34]) on the side of the cell membrane with a green beam that propagates downward from a vertically oriented microscope objective. Directly illuminating the target with the vertical green beam will result in deformations to the beam due to the cell interface and also create non-localized illumination. In this scenario, the bent waveguide can potentially serve two desirable functions: (1) redirecting the green light sideways to the cell membrane and (2) modifying the beam characteristics *in situ*, e.g., to produce a more tightly confined green beam at its tip as compared to the incoming beam.

Three-dimensional waveguide structures, including optical trapping handles, may be fabricated by two-photon polymerization using femtosecond lasers. Femtosecond laser-induced refractive index changes have been used to fabricate waveguides within the volume of transparent materials [32, 33]. These fixed waveguides tend to have low numerical aperture – e.g. for Corning glass (n_{glass} = 1.52), the refractive index step is typically ~1.4×10^{-3} [33], which yields a numerical aperture,

$$NA = \sqrt{n_{waveguide}^2 - n_{background}^2} \approx 0.065. \quad (1)$$

In contrast to these low-NA fixed waveguides, free-standing waveguides fabricated via multiphoton processes can potentially achieve higher numerical apertures by choosing a working environment where they have a higher refractive index contrast with the surrounding medium. For example, immersing photopolymerized SU8 waveguides (n = 1.6 at λ=532nm) in water (n=1.33) will have numerical aperture NA = 0.89. Thus, such waveguides can be strongly guiding (weakly guiding condition: $NA^2 << 2\ n_{background}$). This is important since, owing to their microscopic dimensions, the waveguide would have a rather small bending radius, which could cause losses in the guided modes. We performed finite-difference time domain (FDTD) simulations [35] to visualize the effects to be expected in this case.

2.1 FDTD simulations of optical guiding through the structures

The FDTD simulations were performed on a 2048 × 1024 grid. We used 20nm grid spacing, which ensures sufficient sampling within the waveguide, with at least 16 grid points per wavelength for illumination with 532nm (vacuum wavelength), and up to 33 grid points per wavelength for 1064nm illumination. The simulations all yielded convergent results. The refractive indices used were based on water's dispersion curve reported in [36] and SU8's dispersion curve in [37]. For simplicity in the model, the structure and fields are assumed to be invariant along the z direction. With this assumption, the simulations used fields that are

#158363 - $15.00 USD Received 21 Nov 2011; revised 2 Jan 2012; accepted 4 Jan 2012; published 13 Jan 2012

transverse magnetic to z (our simulations using transverse electric to z showed similar behavior). We started with a simulated light source: a Gaussian with uniform phase, beam waist = 1μm, and 532nm vacuum wavelength. We examined its propagation through a bent, step-index dielectric waveguide assumed to be polymerized SU8 immersed in water. The refractive index Fig. 1(a) shows the time-averaged intensities of the light propagation through the waveguide obtained after 6144 time steps (the time evolution is shown in Media 1).

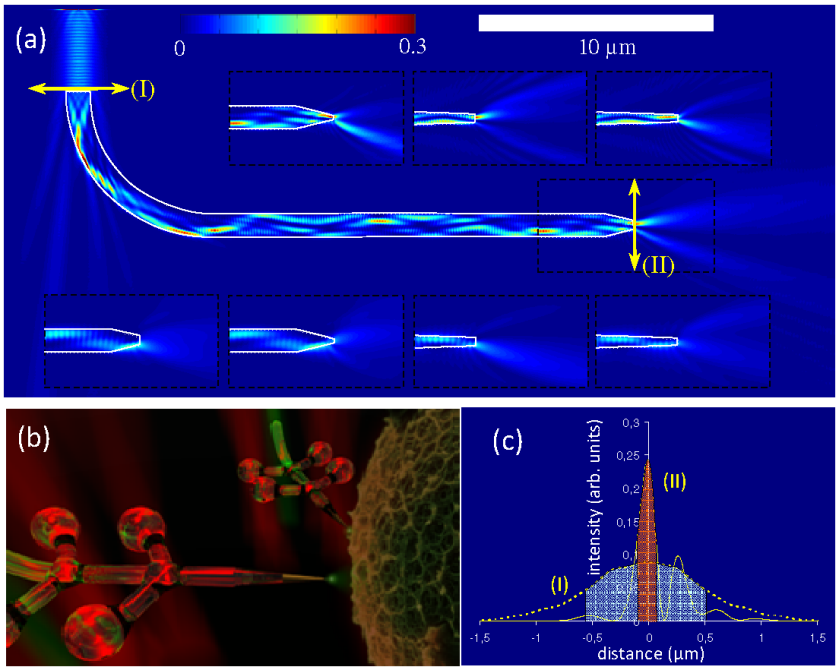

Fig. 1. Redirecting and confining light from far-field optics to a localized target. (a) FDTD model of propagation (λ = 532nm) through a bent polymer waveguide (SU8, n=1.6; bend radius, R = 5.8μm) that is immersed in water (n=1.33). Insets show the field near the tip for different tapers and illumination wavelengths (top: λ = 532nm; bottom: λ = 1064nm. The simulated tips can have abrupt tapers that start ~2μm before the tip or gradual tapers that start right after the bend and appear as slender tips in the insets. The end of the tips are flattened with widths measuring ~0.1μm to ~0.4μm) The time evolution is shown in Media 1 (b) Artist rendition to illustrate the trapping and waveguiding geometry: the bent waveguide redirects vertical light beams onto a target located on the side of a 3D target. (c) Intensity linescans along the dashed lines in (a) show that light exiting the tip (solid line, II) is narrower and has higher peak intensity than the incoming light (dashed, I). The FWHM's are illustrated by the shaded regions.

The waveguide width, D = 1 μm, was chosen to match original Gaussian width and matches the full-width (FWHM) of the incoming beam at the waveguide entrance (see the incoming beam intensity linescan in Fig. 1(c)). The waveguide width, D, numerical aperture, NA = 0.89, and the wavelength, λ = 532 nm determine the normalized waveguide parameter,

$$V = \frac{D\pi}{\lambda} NA = 5.26. \quad (2)$$

A straight waveguide having these parameters will support multimode operation (the single-mode condition, V < 2.405 [38], is achieved at wavelengths λ > 1130 nm). However, this would not necessarily mean a multimode output from the bent waveguide considered here due to its small bending radius (R = 5.8 μm).

The simulation results in Fig. 1(a) show that the beam develops a narrow intense peak once the beam enters the waveguide. The beam encounters some leakage loss at the bend, but most of it is guided further, albeit with reduced peak intensity as the beam propagates through the horizontal section. However, the peak intensity rises again when the beam enters the

#158363 - $15.00 USD Received 21 Nov 2011; revised 2 Jan 2012; accepted 4 Jan 2012; published 13 Jan 2012

tapered end. This allows a narrow intense peak to be coupled out of the tip, which then quickly spreads as diffraction effects set in. Hence, the light coupling out of the tip exhibits higher peak intensity and tighter light confinement compared to the incoming light (see the comparison of the linescans in Fig. 1(c)). While the incoming beam width can be produced by NA~ 0.5 air-immersed objective, reproducing the same FWHM as the outgoing light will require using an immersion objective having NA~ 1.25.

The two functions – redirecting incident vertical light sideways and producing a more intense and tightly confined light at the tip – are also observed when using other tip tapering profiles for a green beam, λ=532nm (see lower insets, Fig. 1(a)). The upper insets of Fig. 1(a), which depict time-averaged fields near the tip when using λ = 1064 nm, show that the same waveguide can be reused for light having longer wavelengths.

2.2 Two-photon microfabrication

In preparation for proof-of-principle experiments demonstrating optically trapped waveguides, we designed and fabricated test waveguides using the two-photon microfabrication system described in [39]. The procedure includes a two-minute soft bake of spin-coated photoresist layer (SU8 2007, Microchem) at 95°C on a hot plate, followed by scanning focused laser illumination and 10-minute post-illumination bake (also at 95°C). Microstructures were formed by scanning tightly focused ultrashort pulses from a Ti:sapphire laser (λ=796μm, 100 fs pulses, 80 MHz repetition rate, 3 mW average power) in the photoresist. The laser pulses were focused by an oil-immersion microscope objective (100× Zeiss Achroplan, 1.25NA objective; DF-type immersion oil Cargille Laboratories, formula code 1261, n=1.515). The focal spot was scanned relative to the resin at speeds of 10μm/s for the spheres and 5μm/s for the connecting rods and tip to solidify voxels with minimum transverse and axial feature sizes of 0.4 ± 0.1μm in transverse and 1 ± 0.1μm in longitudinal directions, respectively.

Some representative SEM images of the fabricated structures are shown in Fig. 2. Figures 2(b)-2(d) illustrate the variety of tip profiles that can be fabricated using the 2PP system. We have iterated through several design/fabrication cycles, where we used optical trapping/waveguiding test results to improve later designs. The representative SEM image shown in Fig. 2(a) shows one of the later designs, where a bent waveguide sits atop a supporting structure that contains spheroidal optical trapping handles. Here, the use of two connecting rods to the waveguide (as opposed to 4 rods for the structures in Fig. 2(b)) minimizes the deformations along the waveguide that can lead to leakage. The reversed angled connecting rods also minimize light coupling out through the rods as opposed to forward-angled connecting rods (e.g., see Fig. 2(c)).

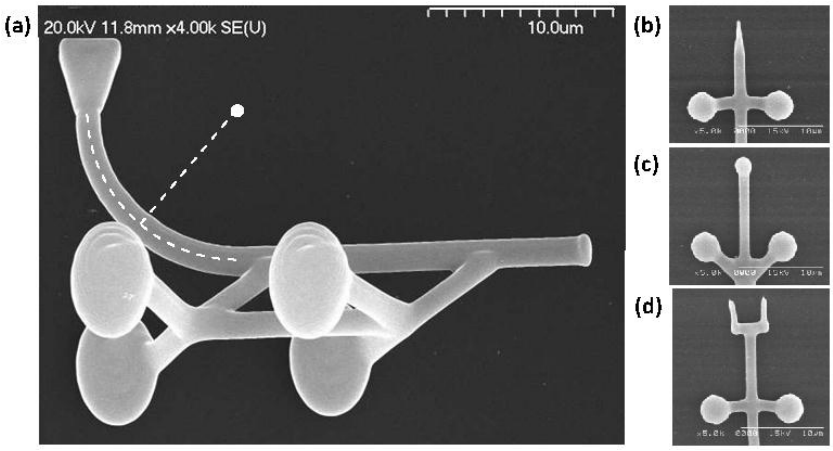

Fig. 2. SEM images of representative two-photon polymerized structures: a) A bent waveguide (bending radius R~8 μm; width ~ 1.5 μm) sitting atop a supporting structure having spheroidal handles for optical trapping; the waveguide is connected via reverse-angled rods for minimal light-coupling loss the support structure; b) – d) Some tip structures that can be fabricated

#158363 - $15.00 USD Received 21 Nov 2011; revised 2 Jan 2012; accepted 4 Jan 2012; published 13 Jan 2012

2.3 Sample preparation

The structures polymerized on the glass substrate stayed in place after their development. Their collection was carried out in a Petri dish filled with the aqueous solution of 0.5% Tween 20 and 0.05 % azide. The structures were first detached from the mechanically fixed substrate by a glass capillary tube tapered to sub-micrometer thickness, then collected into another tapered capillary through an opening of around 50 micrometer by suction with a syringe. The structures were collected with about 5 microliter solvent and transferred into a plastic Eppendorf tube. The collection-transfer efficiency was about 80 percent.

After developing and harvesting, the microstructures were stored in solvent containing water mixed with 0.5% surfactant (Tween 20) and 0.05 % azide. The surfactant prevents the microstructures from sticking to other structures and to the sample chamber while the azide prevents microbial growth during storage. Before using the microstructures, the sample is centrifuged to let the structures settle to the bottom and then briefly sonicated to dislodge any sticking structures for easier collection. The collected structures are first mixed with a fluorescent calcium indicator (10μm calcium orange diluted in ethanol) to enable the visualization of the light propagation. In some cases, the structures are mixed with a dilute solution of dyed microspheres. Upon loading the samples into a cytometry cell (Hellma 131.050, 250μm × 250μm inner cross-sections, 1.6 μL volume), the cells were sealed to reduce evaporation and allow repeated experiments over several days.

3. Guiding light through optically trapped waveguides

3.1 Optical micromanipulation

We used our BioPhotonics Workstation [40] (see schematic illustrated in Fig. 3(a)) to optically trap and manipulate the fabricated waveguides to perform proof-of-principle experiments demonstrating the optical manipulation of free-standing optical waveguides. The BioPhotonics Workstation uses a beam modulation module to create multiple beamlets from an expanded NIR light source (λ=1064nm). Two independently addressable regions in a computer-controlled spatial light modulator create a matched set of counterpropagating beam traps that are projected to the sample through opposite microscope objectives (Olympus LMPlan50×IR, WD=6.0 mm, NA=0.55). The use of lower-NA (as opposed to single-beam optical tweezer systems) opens ample space for inserting a 4.2 mm thick sample chamber (Hellma, 250μm × 250μm inner cross section) and a side-view microscope. We can use the beam modulation module to create a beamlet (λ=1064nm) to be coupled into the waveguide. Moreover, we also introduced a second computer-controlled light source (λ=532nm) through the dichroic mirror that simultaneously couples white-light for top-view imaging. A program developed in LabVIEW handles the interface with the imaging, optical trapping and electronic hardware. A graphical interface streams videos from the top- and side-view microscopes simultaneously and allows the user to control the trapping beams to manipulate the fabricated structures using a mouse or joystick in real-time.

#158363 - $15.00 USD Received 21 Nov 2011; revised 2 Jan 2012; accepted 4 Jan 2012; published 13 Jan 2012

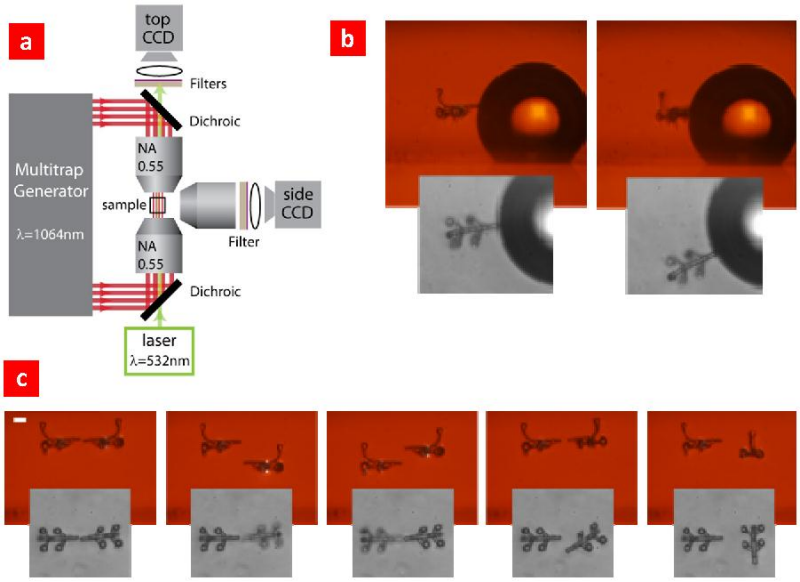

Fig. 3. Experimental setup and optical micromanipulation. (a) Schematic of the experimental setup showing the counterpropagating beam traps, top- and sideview microscope and light coupling. (b) Experimental snapshots showing a 2PP-structure being optically manipulated around a relatively large bubble (~80μm). (c) Snapshots from simultaneous optical manipulation of two microstructures (Media 2). (scalebar:10μm)

During initial experiments, we tested the optical manipulation of the 2PP-fabricated 3D structures. Figures 3(b)-3(c) show concurrent top- and side-view snapshots from some of these experiments. Figure 3(b) mimics the trapping geometry illustrated in Fig. 1(b) and shows a fabricated microstructure being steered around a larger structure (~80μm diameter). Figure 3(c) shows the simultaneous optical trapping and manipulation of two microstructures.

3.2 Light coupling through waveguides held and manipulated by optical traps

To test whether the fabricated structures can indeed act as waveguides, we trapped structures with counterpropagating NIR-beams using their spherical handles, rotated them to point towards the sideview microscope, and then held them in place while an external vertical beam was directed towards the input end of the waveguide. Figure 4 shows snapshots from these experiments. Figure 4(a) shows images from the sideview microscope, which show light of different wavelengths (532nm and 1064nm) emerging from the subwavelength tip. The structures are optically trapped in fluorescent media (10μm calcium orange in ethanol). The 532nm illumination (Laser Quantum's Excel) was coupled into the waveguide by shining a 1.5mm Gaussian beam through the 0.55NA objective lens of the BioPhotonics Workstation and then using the sideview fluorescence image as guide for centering the waveguide entrance within the focused beam's Rayleigh range. The 1064nm illumination was coupled into the waveguide by creating a NIR trap (a circular flattop) near the waveguide entrance. Filtering the green light reveals that the coupled light emerges from the tip with sufficient intensity to excite fluorescence in the surrounding medium.

To test whether the experiments correspond to the numerically simulated results, we rotated the trapped structures to be able to view them sideways. The surrounding fluorescent medium enabled us to visualize the light propagation, as shown by the side-view image in Fig. 4(b). We can see that the propagation qualitatively agrees with the features observed in the simulated propagation. For example, the light emerging from the subwavelength tip would, expectedly, have a narrower width than the rather broad incoming beam. We can also see the losses near the bend and the pronged light pattern emerging from the tip, which we saw in the FDTD simulations. Figure 4(e) also illustrates the possibility for on-the-fly modification of the emerging light – i.e., positioning other optically trapped microscopic optical elements at

#158363 - $15.00 USD Received 21 Nov 2011; revised 2 Jan 2012; accepted 4 Jan 2012; published 13 Jan 2012

the tip. Here we trapped a microsphere and used it as a microlens to focus the divergent light emerging from the tip (An optically trapped microbead was previously used as lens for submicron fabrication in the near-field focus of another laser beam [41]). If needed, different tip designs may be explored in the future for controlling the transverse profile of light emerging from the tip.

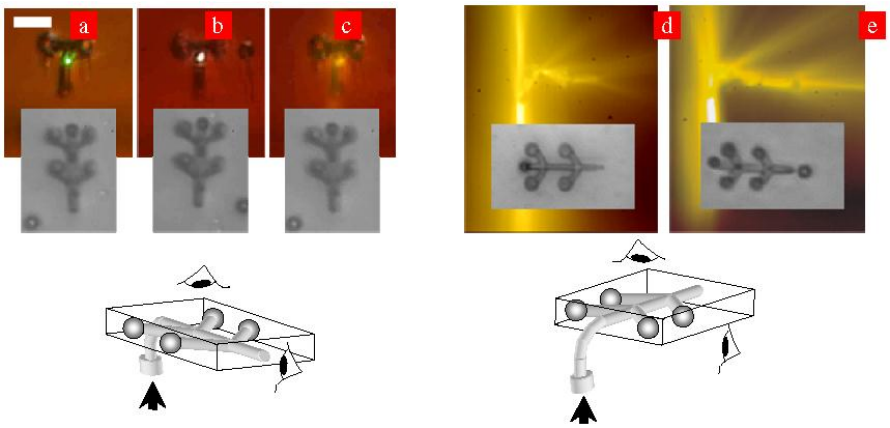

Fig. 4. Guiding light through waveguides held by stationary optical traps. Snapshots from side-view microscopy (Media 3) during light coupling experiments through an optically trapped structure showing (a) λ=532nm; (b) λ=1064nm; (c) fluorescence at 532nm excitation as the waveguide points towards the microscope. (d) and (e): Fluorescence images at 532nm excitation when the waveguide is reoriented to visualize the beam propagation. Light emerging from the tip exhibits a pronged pattern, (d), which can be focused by using an optically trapped bead as lens, (e). (scalebar:10μm)

Waveguides held by stationary optical traps can be used for targeted light delivery by mechanically scanning the target into place (similar to scanning a focal spot in a volume by moving the sample). We also tested the alternative geometry for targeted light delivery, which keeps the target stationary and uses dynamic traps to scan the waveguide. Figure 5(a) shows sideview snapshots from experiments where green light is redirected and guided by a structure that is being optically steered to simulate vertical scanning. Like in the static case, light is guided through the bend and the emerging light excites narrower fluorescence regions as compared to the incoming vertical illumination.

The simulations and experimental results imply that the structure can enable us to use relatively broad beams in the focal volume of low-NA objectives and then redirect them as sharper intensity peaks that can be steered to provide localized optical illumination. As further proof-of-concept demonstration, we trapped a vertical column of dyed microbeads (3μm Polybead® dyed blue) and showed that we can use the steerable waveguide to redirect a broad vertical beam and selectively excite fluorescence from a single microbead located within the column (see Fig. 5(b)). This would have been problematic using direct vertical illumination since the other beads will also be illuminated and distort the beam. We also trapped a 2×2 vertical arrangement of microbeads and demonstrated selective excitation of single beads. These results illustrate that the structure can redirect optical energy from an external source towards a user-defined localized target.

Finally, we tested the possibility of using the structure to guide optical waves in the reverse direction, where light entering the tip is redirected towards the top-view microscope, for possible future use for probing localized fields. Figure 5(c) shows snapshots from proof-of-principle experiments demonstrating the possibility for such reverse coupling. Here we used a trapped waveguide to generate a local field at its tip and then optically manipulated a second waveguide to scan and sense this field. The results show that the waveguide can redirect the localized field, which propagates off-axis beyond the microscope objective's acceptance angle, and enable its detection using low-NA top-view optics. Moreover, it is also

#158363 - $15.00 USD Received 21 Nov 2011; revised 2 Jan 2012; accepted 4 Jan 2012; published 13 Jan 2012

worth noting that the same experiment also shows a precursor experiment for optically reconfigurable optical microcircuits, which currently consists of free-standing waveguides.

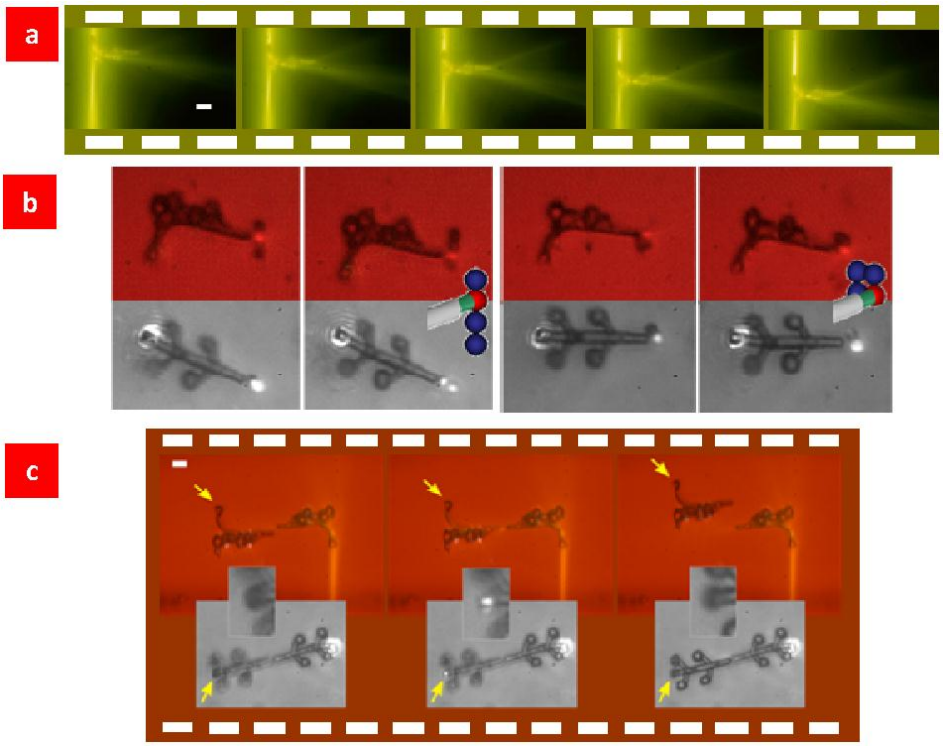

Fig. 5. Light coupling through a dynamically manipulated waveguide. (a) Snapshots from sideview fluorescent imaging of an optically trapped and manipulated waveguide (Media 4). (b) Snapshots showing selective fluorescence excitation of a target bead among a group of beads (left: vertical column of beads; right: 2×2 vertically arranged beads). (c) Snapshots showing reversed light coupling: an optically trapped structure creates a localized field and a second trapped structure is manipulated to scan the local field; the reverse-coupled light is visible from the top microscope (Media 5). The yellow arrow indicates where the light couples out when the scanning tip detects an optical field (scalebar:10μm)

4. Conclusions and outlook

We have performed simulations of light coupling through microfabricated bent waveguides. In our experiments, the waveguides were fabricated using two-photon polymerization and form part as free-standing microstructures that, hence, can be positioned and oriented arbitrarily in a sample using optical traps. The experiments qualitatively reproduce the simulated results of beam redirection and pronged light coupling out of the waveguide tip. The combination of waveguiding with optical trapping and micromanipulation enables the dynamic routing and targeted delivery of optical energy. Moreover, the high-NA waveguide can emit more tightly confined light and we have shown that these waveguides can tap energy from a relatively broad beam and then redirect onto a smaller spot for a more localized photo-excitation e.g., fluorescence, which would otherwise not be possible using the broad, diffraction-limited beam from the low-NA microscope objective. Hence, our proof-of-principle experiments could point to a new paradigm of structure-mediated access beyond the diffraction limit, where our free-standing waveguides form part of a new class of structures– micro-to-nano couplers– that takes in diffraction-limited beams from far-field optics and then reshapes and redirects them for delivering optical force and energy onto nanoscale targets, and vice versa (i.e., nano-to-micro coupling). This effectively mimics a manoeuvrable subwavelength light source and provides a practical alternative to developing a tunable subwavelength light source [18] by shifting the engineering requirements to more manageable

#158363 - $15.00 USD Received 21 Nov 2011; revised 2 Jan 2012; accepted 4 Jan 2012; published 13 Jan 2012

macroscopic laser systems. The known geometry of the structure enables one to pinpoint the nanotip location, even with low resolution imaging, by inferring its position from the easily tracked micron-sized platform. This approach can be adapted to address the challenge of real-time, optical manipulation of nanotools. The viability of a micro-to-nano coupling paradigm is reflected in recent optical probing studies [22–25] showing that the nanotip mechanics (such as position statistics and mechanical forces) can be inferred from the convenient observation of their microscopic handles.

This work exploits a convergence of various contemporary photonic technologies ranging from light-based fabrication and mechanical manipulation to optical guiding for light delivery and probing. Thus, it is fertile ground for interfacing with other photonic technologies for enabling novel functionalities. Future improvements on our free-standing waveguides can tap relevant technologies within chemical functionalization, nanotapered fibers [42] and plasmonics [43] to adapt techniques for controlling the emission or detection through the structure's nanotip. Exploiting plasmonic effects [43] can achieve extreme confinement for localized excitation, precision materials processing and targeted photochemical triggering. Potential applications include manipulation and control of tip-attached nanodevices including, among others: chemically functionalized sensors and probes; metallic nanostructures and metamaterials for plasmonic control and manipulation of the emitted light [43]; crystalline and semiconductor nanowires for generating coherent light [17]; and adapting other light management functions such as 3D-maneouvrable Tip-Enhanced Raman Spectroscopy [44]. It would also be interesting to exploit nonlinear optical effects in the structure to incorporate built-in optical devices like light sources [45, 46]. It would also be worth considering whether we can exploit nanofluidics [47] to extend the micro-to-nano coupling approach for material transport. Besides its generic appeal in nanotechnology, this can be interesting in the life sciences, where control over nanoscale processes promises to accelerate biomedical explorations and innovations.

Acknowledgments

This work was supported by the Danish Technical Scientific Research Council (FTP), the Hungarian Scientific Research Fund (OTKA-NK-72375). We thank B.A.L. Rao for assistance in the sample preparation and E. Mihalik for the SEM images of the microtools.

#158363 - $15.00 USD Received 21 Nov 2011; revised 2 Jan 2012; accepted 4 Jan 2012; published 13 Jan 2012